Princeton University

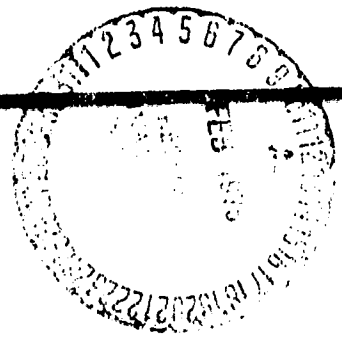

Department of Aerospace and Mechanical Sciences

FINAL TECHNICAL REPORT

HIGH SPEED HYDROGEN/GRAPHITE INTERACTION

Authors: A. J. Kelly, R. Hamman,
O. P. Sharma and D. T. Harrje

Research Supported Under
NGR - 31-001-230

Technical Monitor: Francis C. Schwenk
Atomic Energy Headquarters

Approved by: David T. Harrje
David T. Harrje
Principal Investigator

Approved by: William A. Sirignano
William A. Sirignano
Principal Investigator

May 1974

AMS Report No. 1206

Guggenheim Laboratories for the Aerospace Propulsion Sciences
Department of Aerospace and Mechanical Sciences
PRINCETON UNIVERSITY
Princeton, New Jersey

TABLE OF CONTENTS

I N T R O D U C T I O N

The following sections of this final report on high speed hydrogen/graphite interaction deal with the various aspects of the research program.

Section 1 concerns the theoretical predictions of hydrogen/graphite erosion rates. Our previous report[1-1] covered this topic area in some detail, however, this phase of the research is continuing under Dr. Sharma's direction and a brief summary of the activities are included in this section.

Section 2 describes high temperature, nonequilibrium hydrogen flow in a nozzle. In this section some detail as to computer programs and subroutines is supplied in order to calculate flow characteristics of nuclear rocket applications. The analysis includes subsonic, transonic and supersonic regimes together with equilibrium and non-equilibrium considerations.

Section 3 describes the molecular beam studies of hydrogen/graphite erosion. This phase of the research has concluded. The findings, together with a description of the approach and experimental apparatus,are summarized here.

SECTION 1

THEORETICAL PREDICTIONS OF HYDROGEN/GRAPHITE EROSION RATES

A theoretical model is developed to predict the erosion rate of graphite coating by a stream of hydrogen gas. It is based on a phenomenological description of turbulent reacting boundary layer flow. It also takes into account the effect of lateral curvature in the nozzle as well as the dissociation of hydrogen gas.

The basic conservation equations with the relevant boundary conditions for this model were summarized in the last report[1-1]. The formulation of the problem was done by considering the multicomponent diffusion of species. The detailed description of the transport properties needed for the solution of the equations as well as the transformed forms of the governing equations were also given in the last report[1-1].

A numerical solution is being sought for the set of coupled nonlinear partial differential equations. For this purpose, we are following the general procedure adopted by Herring and Mellor[1-2] for calculating the boundary layer flow of a single component (non-reacting) mixture. Using the Crank-Michelson scheme, the partial differential equations have been transformed into finite difference equations which are then being solved by Gaussian elimination procedure. The expressions are too lengthy for presentation in this report.

There are essentially three successive phases involved in the complete solution of this problem:

(a) The flow external to the boundary layer must be known. This task was undertaken by Mr. R. Hamman who provided the numerical data for the non-equilibrium flow field with a given nozzle geometry by neglecting the boundary layer effects (see Section 2). The choice of step-size along the axial direction is consequently restricted by this input data.

(b) In order to solve the governing equations step by step along the axial direction, we use approximate turbulent similarity flow equations at the initial station. Herring and Mellor generalized the results obtained from incompressible equilibrium turbulent boundary layer flow studies to get approximate compressible turbulent similarity flow equations. In the present analysis, we make use of the same prescriptions for the momentum conservation equation expressed in terms of temperature in contrast to enthalpy. Moreover, the same concept is extended to the species conservation equation.

It must be pointed out that since we have included the dependences on temperature and composition for the various physical properties of the mixture, the final expressions are far more complex, and the logic of the computer program also becomes very involved.

(c) Having obtained the results for the similarity flow, the calculations can be easily completed for other stations by considering the general form of the governing equations. No essential difficulty can be expected at this stage. All the relevant details have been worked out.

In view of the unexpected change of location of the in-

vestigator for this phase of the program, Dr. O. P. Sharma, and the necessity of using a smaller computer facility (IBM 7044), the debugging of the Fortran has been rather slow. It is anticipated that the computation will be completed by summer 1974 at no additional expense to the contract.

SECTION 2

HIGH TEMPERATURE, NONEQUILIBRIUM HYDROGEN FLOW IN A NOZZLE

2.1 Analysis

The analysis is composed of three rather distinctive flow cases: subsonic one dimensional flow, transonic flow and supersonic axisymmetric flow. Only a rough outline of the respective theories is given. For more detailed information one is referred to the references for this section.

The subsonic flow analysis consists of a pressure defined one-dimensional non-equilibrium analysis as given in Refs.2-1 & 2-2. Insufficient reliable information was known to warrant a computer program on a two-dimensional axisymmetric treatment of the subsonic flow.

In the case of transonic flow a model is chosen for a simple, more geometrical treatment analogue to that discussed in Reference 2-2 which gives accurate results compared to experiments. An extensive treatment of the transonic axisymmetric case is given in Reference 2-2, but was rejected for this program as being too complicated.

The analysis of the axisymmetric non-equilibrium supersonic flow employs a method of characteristics solution for the partial differential equations. The finite difference scheme chosen stems from Reference 2-4, being a more simple method than that used in Reference 2-5.

2.1.1 Subsonic one-dimensional flow

The governing differential equations for one-dimensional flow with chemical non-equilibrium are

$$\rho A w = \text{constant} \qquad \text{(continuity)} \qquad (2.1)$$

$$\rho w \frac{dw}{dx} + \frac{dp}{dx} = 0 \qquad \text{(momentum)} \qquad (2.2)$$

$$h + \frac{1}{2}w^2 = \text{constant} \qquad \text{(energy)} \qquad (2.3)$$

$$\frac{d\alpha}{dx} = \frac{\omega}{w} \qquad \text{(chemical relaxation)} \qquad (2.4)$$

In case of chemical equilibrium equation (2.4) is replaced by

$$\alpha = \alpha_e(p,T) \qquad (2.5)$$

or in case of frozen flow by

$$\alpha = \alpha_0 = \text{constant}$$

In the discussion we will not consider the frozen case, as its method of solution is almost identical to the one for equilibrium flow.

As the set of equations both in the equilibrium and in the non-equilibrium case are to be integrated through the transonic region, the area ratio cannot be used as the independant variable because the area ratio defined set of equations is singular at the sonic point.

Using the velocity or pressure as the independant variable has the extra advantage that the set of four differential equations, which originally required simultaneous integration, is reduced to a set of three equations. With the flow field the corresponding area ratio can be computed afterwards.

In the non-equilibrium case there exists a coupling of the equations with the area ratio by means of the chemical relaxation equation. This case will have to be solved by iteration of the complete subsonic flowfield until the computed area ratio converges to the area ratio defined by the nozzle shape.

2.1.1.1. Equilibrium flow

Using velocity as the independant variable equations (2.2) and (2.3) can be written

$$\rho w\, dw + dp = 0 \qquad (2.6)$$

$$dh + w\, dw = 0 \qquad (2.7)$$

Equation (2.4) is replaced by the condition for equilibrium $\alpha = \alpha_e(p,T)$. As the enthalpy h is a function of α and T only

$$dh = h_T\, dT + h_\alpha\, d\alpha$$

where

$$h_T = \left(\frac{\partial h}{\partial T}\right)_\alpha$$

$$h_\alpha = \left(\frac{\partial h}{\partial \alpha}\right)_T$$

Combining this result with (2.5)

$$dh = h_T\, dT + h_\alpha \left[\frac{\partial \alpha_e}{\partial p}\, dp + \frac{\partial \alpha_e}{\partial T}\, dT\right]$$

which reduces the set of equations to

$$\rho w\, dw + dp = 0$$

$$\left(h_\alpha \frac{\partial \alpha_e}{\partial T}\rho + h_T\right) dT + \left(1 - h_\alpha \frac{\partial \alpha_e}{\partial p}\rho\right) w\, dw = 0 \qquad (2.8)$$

Writing this in finite difference form with the velocity as the independant variable

$$\Delta p = (-\rho w)\,\Delta w \qquad (2.9)$$

$$\Delta T = \left(\frac{h_\alpha \frac{\partial \alpha_e}{\partial p}\rho - 1}{h_\alpha \frac{\partial \alpha_e}{\partial T} + h_T}\, w\right)\Delta w \qquad (2.10)$$

which combined with the condition for chemical equilibrium

$$\alpha = \alpha_e(p,T)$$

gives a solution for the equilibrium flow properties.

The coefficients in (2.9) and (2.10) are taken to be the average values between two consecutive points, while the density ρ is computed using the equation of state

$$\frac{p}{\rho} = \frac{kT(1+\alpha)}{2m_H} \qquad (2.11)$$

The local frozen speed of sound can be found using the equation given in appendix A.

As the mass flow $\dot{m}$ is constant, it follows from

$$\rho A w = \dot{m}$$

that at the throat, where $A = A^* = A_{min}$, ρw should take a maximum value. After location of this maximum, the throat properties and the equilibrium mass flow can be determined, and the area corresponding with every set of properties p, T, α and w is known:

$$\dot{m}_{eq} = (\rho w)_{max} A^* \qquad (2.12)$$

and

$$A_n = \frac{\dot{m}_{eq}}{(\rho w)_n} \qquad (2.13)$$

An expression for the nozzle shape links the area with the axial coordinate, which permits us to use the functions

$$p = p_{eq}(x)$$
$$w = w_{eq}(x)$$
$$T = T_{eq}(x)$$
$$\alpha = \alpha_{eq}(x)$$

and all derived equilibrium properties, whenever they are needed.

2.1.1.2. Non-equilibrium flow

As the pressure is relatively insensitive for non-equilibrium effects, it is convenient to use it as the independant variable in the kinetic analysis.

Equations (2.2), (2.4) and (2.3) can be written

$$(\rho w)\,dw + \left(\frac{dp}{dx}\right)dx = 0$$
$$d\alpha - \left(\frac{\omega}{w}\right)dx = 0$$
$$h_T\,dT + \left(h_\alpha \frac{\omega}{w} - \frac{1}{\rho}\left(\frac{dp}{dx}\right)\right)dx = 0$$

or

$$dw = \left[\frac{-1}{\rho w}\left(\frac{dp}{dx}\right)\right]dx$$

$$d\alpha = \left[\frac{\omega}{w}\right]dx$$

$$dT = \left[-\frac{h_\alpha}{h_T}\frac{\omega}{w} + \frac{1}{\rho h_T}\left(\frac{dp}{dx}\right)\right]dx$$

The pressure and its derivatives are assumed to be known; as a first approximation is taken to the equilibrium pressure distribution.

A fourth equation can be derived by differentiating the equation of state (2.11)

$$d\rho = \left[\frac{1}{p}\left(\frac{dp}{dx}\right) - \frac{1}{T}\frac{dT}{dx} - \frac{1}{1+\alpha}\frac{\omega}{w}\right]\rho\,dx$$

These four equations can be rewritten, as shown in appendix A, in the form

$$\frac{dw}{dx} = f_1 - \frac{1}{gw}\left(\frac{dp}{dx}\right) \tag{2.14}$$

$$\frac{d\alpha}{dx} = f_2 = \frac{\omega}{w} \tag{2.15}$$

$$\frac{dT}{dx} = \left[\frac{\gamma-1}{\gamma p}\left(\frac{dp}{dx}\right) - B\right] T \tag{2.16}$$

$$\frac{dg}{dx} = \left[\frac{1}{\gamma p}\left(\frac{dp}{dx}\right) - A\right] g \tag{2.17}$$

where

$$B = \frac{h_\alpha}{T h_T} f_2$$

$$A = \frac{f_2}{1+\alpha} - B$$

The integration method is taken from Reference 2-1 with a few minor alterations.

Setting

$$y_1 = w$$
$$y_2 = \alpha$$
$$y_3 = T$$
$$y_4 = g$$
$$k_1 = \Delta w$$
$$k_2 = \Delta \alpha$$
$$k_3 = \Delta T$$
$$k_4 = \Delta g$$

and

$$\beta_{i,j} = \frac{\partial f_i}{\partial y_j}$$

$$\alpha_i = \frac{\partial f_i}{\partial x}$$

four second order integration formulae in the increments of Y_i can be derived of the form

$$k_{i,n+1} = \frac{h_{n+1}^2}{(2h_{n+1}+h_n)h_n}\left[k_{i,n} + \left(f_{i,n} + \alpha_{i,n} h_{n+1} + \sum_{j=1}^{4} \beta_{i,j,n} k_{j,n+1}\right) \frac{h_n}{h_{n+1}} (h_{n+1}+h_n)\right] \qquad (2.18)$$

where

h_l = stepsize for the l^{th} interval.

The function values f_i and the derivatives α_i and $\beta_{i,j}$ are taken at the n^{th} point.

As the last increment before the computed increment has to be known to apply equation (2.18), it is necessary to use a different set of formulae for the starting step of the integration.

The first order variant of equation (2.18) is

$$k_{i,1} = \left(f_{i,0} + \alpha_{i,0} h + \sum_{j=1}^{4} \beta_{i,j,0} k_{j,1}\right) h \qquad (2.19)$$

when applied on the first interval.

The relative error in the increment $k_{i,n+1}$ for the second order method is

$$\Delta k_i = \left| \frac{k_{i,n+1} - 2k_{i,n} + k_{i,n-1}}{3k_{i,n+1} - k_{i,n}} \right|$$

This formula is used to determine the allowable stepsize.

As the error varies as the stepsize squared, the criterion for doubling and halving the stepsize is given as

$$h_{n+2} = h_{n+1} \qquad \frac{\delta}{10} < \Delta k_{i_{max}} < \delta \qquad (2.20a)$$

$$h_{n+2} = \frac{1}{2} h_{n+1} \qquad \Delta k_{i_{max}} > \delta \qquad (2.20b)$$

$$h_{n+2} = 2h_{n+1} \qquad \Delta k_{i_{max}} < \frac{\delta}{10} \qquad (2.20c)$$

where δ is the maximum error allowed.

Equations (2.18) and (2.19) can be written as four linear algebraic equations

$$a_l k_{1,n+1} + b_l k_{2,n+1} + c_l k_{3,n+1} + d_l k_{4,n+1} = e_l$$

$$l = 1,2,3,4$$

which are solved for the increments $k_{i,n+1}$, i=1,2,3,4.

The integration method is only weakly dependant on the engine size and allows an integration step several orders of magnitude larger than the chemical relaxation length.

The gas properties at the throat and the mass flow are determined the same way as treated in the paragraph on equilibrium flow.

$$\dot{m} = (\rho w)_{max} A^*$$

and

$$A_n = \frac{\dot{m}}{(\rho w)_n}$$

A convergence criterion is applied on the mass flow and the one-dimensional computation is ended, when sufficient convergence is achieved. If no sufficient convergence is found, the complete one-dimensional non-equilibrium calculation is restarted, using the newly computed pressure profile.

The form of the functions and derivatives in equations (2.18) and (2.19) is given in Appendix A.

2.1.2. Transonic flow

Basis for the analysis is a modified Sauer analysis as given in Reference 22 by Nickerson. The method employs first order perturbation theory to find

a solution for a constant property line at the throat minimum point.

For a more extensive discussion of the theory use Reference 2-2. Only the results of and changes in that theory will be given here.

The constant property line selected is the isobar at the throat minimum point. The coordinates of the isobar are given by

$$x = \frac{1}{2}(1-r^2)\left(\frac{2R_3}{\gamma+1}\right)^{-1/2} \qquad (2.21)$$

where

R_3 = downstream normalized throat radius of curvature

γ = average specific heat ratio in the throat region

r = radial normalized coordinate

x = axial normalized coordinate.

The average specific heat ratio is determined as

$$\gamma = \frac{1}{2}\left(\gamma^* + \frac{\sum_{i=1}^{n} r_i \gamma_i}{\sum_{i=1}^{n} r_i}\right) \qquad (2.22)$$

where the asterisk denotes the throat property following from the one-dimensional analysis and γ_i is the property at point i on the isobar. n is the total number of points on the isobar.

The spacing of the points on the isobar is determined such that the mass flow through each annular element is equal.

Hence

$$r_1 = 0 \qquad (2.23)$$

$$r_2 = \sqrt{\frac{A^*}{(n-1)\pi}} \qquad (2.24)$$

and

$$r_{i+1} = r_2\sqrt{i} \qquad i = 2, \ldots (n-1) \qquad (2.25)$$

Denoting all one-dimensional throat properties with an asterisk, it follows for the pressure on the isobar

$$p = p^* \left(1 - \frac{\gamma}{4} \frac{1}{R_3 + \frac{\gamma}{4}} \right) \tag{2.26}$$

The axial and radial components of the velocity are

$$u = a^* \left(1 + \frac{r^2}{2} - \frac{1}{4} + \left(\frac{2R_3}{\gamma+1} \right)^{1/2} x \right) \frac{1}{R_3}$$

$$v = a^* \left(\frac{1}{4} \left(\frac{\gamma+1}{2} \right)^{1/2} (r^3 - r) + R_3^{1/2} r x \right) \frac{1}{R_3^{3/2}}$$

Using equation (2.23) these expressions can be simplified into

$$u = a^* \left(1 + \frac{1}{4R_3} \right) \tag{2.27}$$

$$v = a^* \left[\frac{(r - r^3)\left(\frac{\gamma-1}{2}\right)^{1/2}}{4R_3^{3/2}} \right] \tag{2.28}$$

which shows that the axial velocity is constant on the isobar.

The resultant velocity is

$$w = \sqrt{(u^2 + v^2)} \tag{2.29}$$

The streamline angle is found easily by

$$\theta = \operatorname{atan} \left(\frac{v}{u} \right) \tag{2.30}$$

The two other flow properties to be determined are the mass fraction atomic hydrogen and the temperature.

As solving the chemical relaxation equation

$$\frac{d\alpha}{dz} = \frac{\omega}{w}$$

over the relatively large distance from throat to isobar leads to severe

numerical instability for interpolation from the property table provided by the one-dimensional non-equilibrium analysis. The temperature follows from the energy equation

$$h(\alpha, T) = h_0 - \frac{1}{2}w^2 \qquad (2.31)$$

2.3 Description of program subroutines

The program subroutines are divided in four groups

- main program and general subroutines used throughout the computation
- subroutines used for the computation of the one-dimensional subsonic flow
- subroutines for the determination of the transonic line
- subroutines that perform the two-dimensional supersonic flow calculation.

2.4 Main program and supporting subroutines

The subroutines in this group are

MAIN PRØGRAM

SUBRØUTINE CØNSTA

CHEMEQ

EQUIL

GAMMA

TEMP

2.4.1 Main calling program

MAIN PRØGRAM

2.4.2 Input and physical constants

SUBRØUTINE CØNSTA

In this subroutine the physical constants used in the program are initialized and the nozzle shape and case parameters are read in. The variables, used in the internal computation, are derived from the data given in the nozzle shape parameters.

Finally the values of the input parameters are printed.

Physical constants

The physical constants, as they are given in the subroutine, are

- AA constant in the exprssion for the reaction rate FKF= $\frac{AA}{\sqrt{T}}$, where T is the temperature in degrees K.
- FMI mass of a hydrogen atom
- FK Boltzmann constant
- THED characteristic temperature for dissociation of hydrogen
- THEV characteristic temperature for vibration of hydrogen
- PI geometrical constant
- WHY atomic weight of hydrogen

The constants are set at the values

AA = 0.7×10^{18} cm^6 $^oK^{\frac{1}{2}} mole^{-2} sec^{-1}$

FMI = 0.1674×10^{-25} g

FK = 0.138×10^{-17} erg $^oK^{-1} mole^{-1}$

THED = 54733 ^oK

THEV = 6140.0 ^oK

PI = 3.14159

WHY = 1.008 g/mole

- IF (LENGTH.GT.0) it follows through

$$A1 = \frac{REXIT - REE - THEX.\tan(THSUP)}{THEX^2}$$

$$B1 = \tan(THSUP) - 2.A1.XEE$$

that

- XEF = XEE + THEX
- THEX = atan (2.A1.XEF) + B1 (rad)

- IF (LENGTH.EQ.0)

$$- XEF = \frac{2(REXIT - 1 - RTHRE.(1-\cos(THSUP)))}{\tan(THEX) + \tan(THSUP)} + XEE$$

and generally

$$- COL = \frac{(XEF - XEE)\tan(THSUP)}{\tan(THSUP) - \tan(THEX)}$$

The parameters IWALL, IPERF, IPROP, INTER, NPNTS, IOUT and LENGTH determine the case that has to be computed and the shape and quantity of the output.

PROGRAM INPUT — P$\emptyset$ stagnation pressure (dyne/cm^2)

T$\emptyset$ stagnation temperature (^{0}K)

PROGRAM OUTPUT — internal constants

PRINT

CALLING — DATA

SUBRØUTINE EQUIL

CALLED BY — MAIN PRØGRAM

2.4.3 General subroutines

SUBRØUTINE CHEMEQ

EQUIL

GAMMA

TEMP

Nozzle shape parameters

The nozzle shape is assumed to be composed out of circular arcs, straight lines and a parabolic supersonic expansion section.

Read in are

- RCHAM combustion chamber radius
- RØNE nozzle inlet radius of curvature
- RTWØ upstream throat radius of curvature
- RTHRE downstream throat radius of curvature
- RSTAR throat radius (cm)
- REXIT nozzle exit radius
- THSUB maximum nozzle inlet angle (rad)
- THSUP maximum nozzle exit angle (rad)
- THEX IF (LENGTH.EQ.0) nozzle exit angle (rad)
  IF (LENGTH.GT.0) length of parabolic nozzle section

All values, with the exception of RSTAR and the angles, are dimensionless with respect to the throat radius.

The internal nozzle shape parameters, which can be derived

- XBE = RØNE . sin (THSUB)

- XCE = RCHAM - 1 - RTWØ (1 - cos (THSUB)) + $\frac{\text{RØNE}\left(\frac{1}{\cos(\text{THSUB})} - 1\right)}{\tan(\text{THSUB})}$

- XDE = XCE + RTWØ . sin (THSUB)
- XEE = XDE + RTHRE . sin (THSUP)
- RBE = RCHAM + RØNE (cos (THSUB) - 1)
- RCE = 1 + RTWØ (1-COS(THSUB))
- REE = 1 + RTHRE (1 - cos (THSUP))

SUBROUTINE CHEMEQ (T,FKP,DFKP)

This subroutine is used during the complete computation to provide the other subroutines with the value of the equilibrium constant FKP ($(dyne/cm^2)^{\frac{1}{2}}$) and the derivative DFKP ($=\frac{d}{dT}(\ln(FKP))$) at a given temperature T for the reaction $H_2 \rightleftharpoons 2H$.

The first time the subroutine is called two arrays, S and TAB, are read in. Immediately afterwards a flag is set

NFLAG=1

which prevents that the next time, when the subroutine is called, it will try to read the values for S and TAB again. TAB and S are defined

- TAB = $^{10}\log K_p$, K_p in $(atmospheres)^{\frac{1}{2}}$
- S corresponding temperature in degrees K.

and are taken from the JANNAF tables, Reference 2-6. The range of temperatures covered runs from 0^oK until 6000^oK.

At the required value of the temperature T the corresponding value of FKP is found by logarithmic interpolation, and the result is converted to the output units. In the same loop the value of the derivative $\frac{d}{dT}(\ln K_p)$ is determined.

PROGRAM INPUT	T	temperature (^oK)
PROGRAM OUTPUT	FKP	equilibrium constant ($(dyne/cm^2)^{\frac{1}{2}}$)
	DFKP	logarithmic derivative of the equilibrium constant ($(^oK)^{-1}$)
CALLING		DATA
CALLED BY		SUBROUTINE

SUBROUTINE EQUIL (P,T,ALP)

Calculates at given pressure P and temperature T the corresponding value of the mass fraction atomic hydrogen ALP at chemical equilibrium conditions according to the relation

```
ALP=DSQRT(1./(1.+4.*P/(FKP*FKP)))
```

where FKP is the value of the equilibrium constant at T ^{o}K.

PROGRAM INPUT	P	pressure (dyne/cm^2)
	T	temperature (^{o}K)
PROGRAM OUTPUT	ALP	mass fraction atomic hydrogen at equilibrium conditions.
CALLING	SUBROUTINE CHEMEQ	
CALLED BY	SUBROUTINE	

SUBRØUTINE GAMMA (P,T,ALP,GAM,AF2,RHØ)

At given

- pressure P
- temperature T
- mass fraction atomic hydrogen ALP

are computed

- specific heat ratio GAM of the mixture
- squared frozen speed of sound AF2
- density RHØ

according to the expressions (A1), (A7) and (A8) of appendix A.

PROGRAM INPUT	P	pressure (dyne/cm^2)
	T	temperature (^oK)
	ALP	mass fraction atomic hydrogen
PROGRAM OUTPUT	GAM	specific heat ratio
	AF2	squared frozen speed of sound (cm^2/sec^2)
	RHØ	density (g/cm^3)
CALLED BY	SUBRØUTINE	

2.5 Subsonic flow

The subroutines in this group are split in two subsections, the first one dealing with one-dimensional equilibrium flow, the second one with one-dimensional non-equilibrium flow. It contains

SUBRØUTINE CØEQ
CØRTAB
EQUIN
STØUT1
TABLE
CHECK
DERISB
PUNØUT
SØLVE
SUBCØ1
SUBCØ2
SUBEX

2.5.1 Equilibrium flow

SUBRØUTINE CØEQ
CØRTAB
EQUIN
STØUT1
TABLE

SUBRØUTINE CØEQ (P,T,W,ALP,CQ1,CQ2)

The coefficients of the two finite difference equations for integration of the one-dimensional equilibrium flow field (c.f. section 2.1.1.1.; equations (2.9) and (2.10))

$$CQ1 = \varrho w$$

$$CQ2 = \frac{h_\alpha \frac{\partial \alpha_e}{\partial p} \varrho - 1}{h_\alpha \frac{\partial \alpha_e}{\partial T} + h_T} w$$

are computed here. The expressions for the partial derivatives

$$\frac{\partial \alpha_e}{\partial p} \quad \text{and} \quad \frac{\partial \alpha_e}{\partial T}$$

can be found in appendix A (equations (A12a) and (A12b)).

PROGRAM INPUT	P	pressure (dyne/cm^2)
	T	temperature (^{o}K)
	W	velocity (cm/sec)
	ALP	mass fraction atomic hydrogen
PROGRAM OUTPUT	CQ1	coefficient in equation (2.9)
	CQ2	coefficient in equation (2.10)
CALLING	SUBRØUTINE CHEMEQ	
CALLED BY	SUBROUTINE EQUIN	

SUBROUTINE CORTAB (W,X,M,WE,EX,J)

The subroutine modifies a table (W,X) with M entries into a table (WE, EX) with J entries with the result that between each two values of the array EX in the second table a constant interval is constructed.

The interpolation between two values of X is achieved with the formula

$$WE(J) = W(I) \, e^{\left(\ln \frac{W(I+1)}{W(I)}\right)\left(\frac{EX(J)-X(I)}{X(I+1)-X(I)}\right)},$$

$$X(I) < EX(J) < X(I+1)$$

where EX(J)=EX(J-1)+RELL

RELL=.03*RSTART

EX(1)=X(1)

A logarithmic interpolation method is chosen as it represents most accurately the shape of the function W=W(X) between two subsequent points.

PROGRAM INPUT	W	velocity (cm/sec)
	X	axial coordinate (cm)
	M	number of entries in (W,X) table
PROGRAM OUTPUT	WE	velocity (cm/sec)
	EX	axial coordinate (cm)
	J	number of entries in (WE,EX) table

CALLED BY SUBROUTINE EQUIN

SUBRØUTINE EQUIN (PØ,TØ,FMASS,M,X,P,TS,WS,AS,PBEG)

The subroutine computes the equilibrium pressure distribution P as a function of the axial coordinate X and the equilibrium mass flow FMASS.

Two main calculations can be distinguished. After the computation of the initial flow conditions from the stagnation pressure PØ and stagnation temperature TØ, which uses the common expression for the temperature ratio in compressible flow as a function of the Mach number and the specific heat ratio, the energy equation and the condition for chemical equilibrium, a table of the equilibrium gas properties

- velocity W
- pressure P
- temperature T
- mass fraction atomic hydrogen ALP
- density RHØ
- frozen Mach number FMACH

is computed, using the relations described in section 2.1.1.1.

During this calculation the maximum value of the product (RHØ*W) is determined, from which the equilibrium mass flow FMASS follows.

After computation of the sets of gas properties corresponding with the area by applying continuity, follows the construction of a table of the velocity WE as a function of the axial coordinate EX by means of SUBRØUTINE TABLE, which employs an analytic expression for the nozzle geometry. At the same time the nozzle inlet conditions

- pressure PBEG=PS
- temperature TS
- mass fraction atomic hydrogen AS
- velocity WS

SUBRØUTINE STØUT1 (P,T,ALP,RHØ,W,A,X,FMACH)

This subroutine provides the regular output of the results of the one-dimensional performance calculation.

The nozzle area is converted in the area ratio by dividing by (RSTAR*RSTAR*PI). Printed are for all stations

- area ratio A
- axial coordinate X (cm)
- pressure P (dyne/cm^2)
- temperature T (^{o}K)
- density RHØ (g/cm^3)
- mass fraction atomic hydrogen ALP
- velocity W (cm/sec)
- frozen Mach number FMACH

When the frozen Mach number becomes greater than unity, the vacuum specific impulse is computed according to

$$SPI=\frac{1}{981}\left(W+\frac{P}{RH\emptyset*W}\right)$$

and printed.

PROGRAM INPUT	P	pressure (dyne/cm^2)
	T	temperature (^{o}K)
	ALP	mass fraction atomic hydrogen
	RHØ	density (g/cm^3)
	W	velocity (cm/sec)
	A	nozzle area (cm^2)
	X	axial coordinate (cm)
	FMACH	frozen Mach number
PROGRAM OUTPUT	PRINT	
CALLED BY	SUBRØUTINE EQUIN	
	SUBEX	

The table (WE,EX) is corrected with the aid of SUBRØUTINE CØRTAB to ensure an equal stepsize DX in the resulting table (W,X), which furnishes the new input for the second run through the equilibrium flow integration. The final pressure table (P,X) is obtained again with the aid of SUBRØUTINE TABLE.

SUBRØUTINE STØUT1 takes care of the standard print output of the results.

PROGRAM INPUT	PØ	stagnation pressure (dyne/cm^2)
	TØ	stagnation temperature (^{o}K)
PROGRAM OUTPUT	FMASS	equilibrium mass flow (g/sec)
	M	number of entries in the arrays P and X
	X	axial coordinate (cm)
	P	pressure (dyne/cm^2)
	TS,WS,AS	temperature (^{o}K), velocity (cm/sec) and mass fraction atomic hydrogen corresponding with the first entry in the (P,X) table
	PREG	nozzle inlet pressure (dyne/cm^2)
CALLING	SUBRØUTINE CHEMEQ	
	CØEQ	
	CØRTAB	
	EQUIL	
	GAMMA	
	STØUT1	
	TABLE	
CALLED BY	SUBRØUTINE SUBEX	

SUBRØUTINE TABLE (P,A,N,ASTAR,T,W,ALP,X,Q,M,TS,WS,AS,NSTAR)

The property/area table (P,A) with N entries is converted in a property/axial coordinate table (Q,X) with M entries.

The values of the other three one-dimensional flow properties TS, WS and AS corresponding with the first entry in the (Q,X) table are interpolated from the input arrays T, W and ALP. NSTAR is the index of the entries at the nozzle throat.

The relations that link the axial coordinate X with the nozzle area A, non-dimensionalizing the axial coordinate X and the radial coordinate by dividing through the throat radius RSTAR, are:

$$R(J)=\sqrt{A(J)/ASTAR}$$

- if (R(J).LT.RCHAM)

$$X(J)=\sqrt{(R\emptyset NE^2-(R(J)-RCHAM+R\emptyset NE)^2)}$$

- if (R(J).LT.RBE)

$$X(J)=(RCHAM-R(J)+R\emptyset NE(\frac{1}{\cos(THSUB)}-1))\frac{1}{\tan(THSUB)}$$

- if (R(J).LT.RCE)

$$X(J)=XDE-\sqrt{(RTW\emptyset^2-(RTW\emptyset+1-R(J))^2)}$$

- if (J.GT.NSTAR)

$$X(J)=XDE+\sqrt{(RTHRE^2-(R(J)-1-RTHRE)^2)}$$

- if (R(J).GT.REE)

$$X(J)=XEE+C\emptyset L(1-\sqrt{(1-2\frac{R(J)-REE}{E\emptyset L.\tan(THSUP)})})$$

Finally all computed X values are dimensionalized

$$X(J)=X(J).RSTAR$$

PROGRAM INPUT

P,A — gas property/nozzle area table to be converted; A in cm^2

N — number of entries in (P,A) table

		N entries
	NSTAR	index of properties at the nozzle throat
PROGRAM OUTPUT	Q,X	gas property/axial coordinate table; X in cm
	M	number of entries in (Q,X) table
	TS,WS,AS	with (Q(1),X(1)) corresponding values of the arrays T, W and ALP
CALLED BY	SUBROUTINE EQUIN	
	SUBEX	

3.2.2. Non-equilibrium flow

SUBROUTINE CHECK

DERISB

PUNOUT

SOLVE

SUBCO1

SUBCO2

SUBEX

SUBRØUTINE DERISB (P,T,RHØ,ALP,W,DPX,DP2X,F1,F2,F3,F4,F1X,F1W,F1R,F2W,F2R,F2T,F2A,F3X,F3W,F3R,F3T,F3A,F4X,F4W,F4R,F4T,F4A)

This subroutine computes at known

- pressure P
- temperature T
- density RHØ
- mass fraction atomic hydrogen ALP
- velocity W
- pressure first derivative DPX
- pressure second derivative DP2X

the functions F1, F2, F3, F4 and their derivatives with respect to x, w, α, T and ρ, according to the expressions given in appendix A (equations (A13) through (A16) and following), which will be used for the calculation of the coefficients of the first and second order integration methods for one-dimensional non-equilibrium flow.

PROGRAM INPUT	P	pressure (dyne/cm^2)
	T	temperature (^{0}K)
	RHØ	density (g/cm^3)
	ALP	mass fraction atomic hydrogen
	W	velocity
	DPX	pressure first derivative (dyne/cm^3)
	DP2X	pressure second derivative (dyne/cm^4)
PROGRAM OUTPUT	F1,F2,F3,F4 and their derivatives (c.f. appendix A)	
CALLING	SUBRØUTINE CHEMEQ	
CALLED BY	SUBRØUTINE SUBCØ1	
	SUBCØ2	

SUBRØUTINE SØLVE (P,T,RHØ,ALP,W,DX,DPX,DP2X,DWN,DTN,DRN,DAN,DW,DT,DR,DA,NØNE,DX1)

Four linear algebraic equations in four unknowns are solved using Kramer's Rule. The equations are of the form

$$a_i DW + b_i DA + c_i DT + d_i DR = e_i \qquad i = 1,2,3,4$$

and are the rearranged integration formulae from section 2.1.1.2, equations (2.18) and (2.19).

The coefficients a_i, b_i, c_i, d_i and e_i are computed in SUBRØUTINE SUBCØ1 (first order method, applied only for the initial integration interval, if (NONE.EQ.1)) and SUBRØUTINE SUBCØ2 (second order method, used for all subsequent steps).

PROGRAM INPUT

P	pressure at last calculated (n^{th}) point (dyne/cm^2)
T	temperature at n^{th} point (^oK)
RHØ	density at n^{th} point (g/cm^3)
ALP	mass fraction atomic hydrogen at n^{th} point
W	velocity at n^{th} point (cm/sec)
DX	axial distance between n^{th} and $(n+1)^{th}$ point (cm)
DPX	value of $\frac{dp}{dx}$ at the n^{th} point (dyne/cm^3)
DP2X	value of $\frac{d^2p}{dx^2}$ at n^{th} point (dyne/cm^4)
DWN	increment in velocity between $(n-1)^{th}$ and n^{th} point (cm/sec)
DTN	increment in temperature between $(n-1)^{th}$ and n^{th} point (^oK)
DRN	increment in density between $(n-1)^{th}$ and n^{th} point (g/cm^3)

	DAN	increment in mass fraction atomic hydrogen between $(n-1)^{th}$ and n^{th} point
	NØNE	n
	DX1	axial distance between $(n-1)^{th}$ and n^{th} point (cm)
PROGRAM OUTPUT	DW	increment in velocity between n^{th} and $(n+1)^{th}$ point (cm/sec)
	DT	increment in temperature between n^{th} and $(n+1)^{th}$ point (^{o}K)
	DR	increment in density between n^{th} and $(n+1)^{th}$ point (g/cm^3)
	DA	increment in mass fraction atomic hydrogen between n^{th} and $(n+1)^{th}$ point
CALLING	SUBRØUTINE SUBCØ1	
	SUBCØ2	
CALLED BY	SUBRØUTINE SUBEX	

SUBRØUTINE SUBCØ1 (P,T,RHØ,ALP,W,DPX,DP2X,A1,A2,A3,A4,B2,B3,B4,C2,C3, C4,D1,D2,D3,D4,E1,E2,E3,E4,DX)

Computation of the coefficients of the four linear algebraic equations, obtained from the first order integration method, c.f. section 2.1.1.2, equation (2.19).

The values and the derivatives of the functions F1, F2, F3 and F4 at given P, T, RHØ, ALP and W (equations (A13) through (A18), appendix A) are computed in SUBRØUTINE DERISB.

The coefficients A1, A2, etc. are defined

A1=F1W-1/DX

A2=F2W

A3=F3W

A4=F4W

B2=F2A-1/DX

B3=F3A

B4=F4A

C2=F2T

C3=F3T-1/DX

C4=F4T

D1=F1R

D2=F2R

D3=F3R

D4=F4R-1/DX

E1=-F1-F1X.DX

E2=-F2

E3=-F3-F3X.DX

E4=-F4-F4X.DX

PROGRAM INPUT	P	pressure (dyne/cm^2)
	T	temperature (^{0}K)
	RHØ	density (g/cm^3)
	ALP	mass fraction atomic hydrogen
	W	velocity (cm/sec)
	DPX	derivative dp/dx (dyne/cm^3)
	DP2X	derivative d^2p/dx^2 (dyne/cm^4)
	DX	axial interval (cm)
PROGRAM OUTPUT	A1,A2,...,E3,E4	coefficients of linear algebraic equations
CALLING	SUBRØUTINE DERISB	
CALLED BY	SUBRØUTINE SØLVE	

SUBRØUTINE SUBCØ2 (P,T,RHØ,ALP,W,DPX,DP2X,A1,A2,A3,A4,B2,B3,B4,C2,C3, C4,D1,D2,D3,D4,E1,E2,E3,E4,DX,DWN,DTN,DAN,DIN,DX1)

Computation of the four linear algebraic equations, obtained from the second order integration method, c.f. section 2.1.1.2, equation (2.18). The values and the derivatives of the functions F1, F2, F3 and F4 (equations (A13) through (A18), appendix A) are calculated in SUBRØUTINE DERISB.

Setting

$$P=DX1(DX+DX1)/DX$$

$$PQ=DX\frac{(DX+DX1)}{(2.DX+DX1)}$$

the coefficients A1, A2, etc. are defined

$$A1=F1W-1/PQ$$

$$B2=F2A-1/PQ$$

$$C3=F3T-1/PQ$$

$$D4=F4R-1/PQ$$

$$E1=-DWN/Q-F1X.DX-F1$$

$$E2=-DAN/Q-F2$$

$$E3=-DTN/Q-F3X.DX-F3$$

$$E4=-DIN/Q-F4X.DX-F4$$

A2, A3, A4, B3, B4, C2, C4, D1, D2 and D3 have the same definition as in SUBRØUTINE SUBCØ1.

PROGRAM INPUT		
	P	pressure (dyne/cm^2)
	T	temperature (^{o}K)
	RHØ	density (g/cm^3)
	ALP	mass fraction atomic hydrogen
	W	velocity (cm/sec)
	DPX	derivative dp/dx (dyne/cm^3)

DX axial interval between last computed point and next following point (cm)

DWN increment in velocity between last computed point and the point before (cm/sec)

DTN increment in temperature between last computed point and the point before (^{o}K)

DRN increment in density between last computed point and the point before (g/cm^3)

DAN increment in mass fraction atomic hydrogen between last computed point and the point before

DX1 axial interval before DX (cm)

PROGRAM OUTPUT A1,A2,...,E3,E4 coefficients of linear algebraic equations

CALLING SUBROUTINE DERISB

CALLED BY SUBROUTINE SOLVE

3.3 Transonic flow

This group is composed of only one subroutine

SUBROUTINE INLINE

SECTION 3

MOLECULAR BEAM STUDIES OF HYDROGEN/GRAPHITE EROSION

Introduction

As part of its contoured exhaust nozzle, the NERVA solid core nuclear rocket flight engine (Ref.3-1) was designed to incorporate a radiatively cooled graphite skirt. The choice of graphite for this skirt, extending from an area ratio of 24 to 1 to the exit plane (area ratio 100 to 1), rather than the more commonly used refractory metals, was based upon the superior nucleonic properties of low atomic weight graphite as opposed to those of high atomic weight metals. While the thermo-mechanical properties of graphite are quite adequate for its application as a skirt material, there exists however a question of its long term compatibility with the high temperature hydrogen propellant.

It is well established (Ref.3-2,-3,-4) that at high temperature (1000°K) and particularly under conditions of high temperatures and pressures (0 (1) atm) hot graphite will react with hydrogen to form simple hydrocarbons. Such a reaction, if sufficiently vigorous, would have a pronounced effect upon the utility of the nozzle skirt for multiple missions requiring cumulative burn times on the order of 10 hours or so. Consequently, it was deemed of importance to have definitive information available concerning the details of hydrogen-carbon surface reaction under conditions anticipated to be present at the surface of

the skirt during all phases of NERVA engine operation.

The mechanisms by which graphite surfaces react with heated hydrogen have been studied basically under equilibrium conditions. Clarke and Fox (Ref.3-2) employed a filament to investigate the reaction of hydrogen and graphite over a temperature range 2000°K to 3400°K and pressures from 10^{-2} to 1 atms. These experiments, conducted at low total hydrogen flow rates, permitted them to conclude that at temperatures below 3000°K and pressures between 10^{-2} and 1 atms, the rate of reaction at the surface of the graphite is directly proportional to the hydrogen pressure and to the square root of the dissociation constant for this gas. At higher temperatures the sublimation rate of graphite is controlling, and C_2H_2 and C_3H_4 are predominant as reaction products.

Sanders (Ref.3-2) of Lewis Research Center measured weight loss from graphite test samples heated in the range 1820°K to 2430°K at atmospheric pressure. The flow rate of hydrogen was low (47 cm^3/ sec) and equilibrium was maintained throughout the test series. The data collected from these tests at temperatures in excess of 2070°K, correlate quite well with thermodynamic calculations of the equilibrium reaction of carbon and hydrogen. Divergence between the data and computed reaction rates in the temperature range between 1820°K and 2070°K was attributed to a lack of thermodynamic equilibrium induced by the low, but significant, hydrogen flow rate employed during the tests. In addition to predicting the reaction rate, the calculations

indicated that acetylene (C_2H_2) would be the primary reaction product. Earlier, Heddon (Ref.3-4) determined the rate of methane production for graphite reacting with hydrogen at pressures from 10^1 to 10^2 atmospheres and temperatures from 1270°K to 1520°K. It was concluded that the rate determining step in this pressure and temperature regime consisted of hydrogenation of CH_2-CH_2-groups at the graphite lattice coupled with a splitting of the -CH_2-CH_2- bond. It was further concluded that the reaction rate was negligible at temperatures below 1270°K.

These studies, all conducted under equilibrium conditions, have but limited applicability to the problem of establishing the erosion rate of a contoured nozzle. It is necessary, when trying to establish the chemical erosion rate of the graphite nozzle skirt in question, to not only have knowledge of the graphite-hydrogen reaction mechanism, but also to have a fully developed model for the flow field and its interaction with the boundary.

The nozzle skirt under continuous operating conditions will attain an equilibrium temperature which varies as a function of longitudinal position, assuming axial symmetry, and is determined by a balance between the heat flux to the surface through the reacting boundary layer inside and thermal radiation from the outside surface. Consequently, the conditions existing at the graphite-hydrogen interface will be very much different from those maintained in the experiments referenced. In particular, it is difficult to determine the influence surface temperature

has upon the overall reaction rate from, for instance, the effect of hydrogen temperature or velocity. Such information is necessary for the proper development of a coherent model of the reacting boundary layer in the skirt.

A practical engineering assault on the problem of graphite skirt erosion (Ref.3-5,-6) has shown that,on the basis of model tests employing AGCarb- 101 material as a test sample, and pressures and temperatures commensurate with those anticipated to be encountered, erosion rates will be acceptable. Similar tests conducted with helium rather than hydrogen failed to cause erosion. It might be concluded that this is an unambiguous indication of a purely chemical, as opposed to mechanical, erosion mechanism. However, the question can be raised as to whether the surface is not acting as a catalyst for the recombination of the dissociated hydrogen present in the flow leading to intensified reactivity in excess of that to be anticipated from purely thermal considerations. A more extensive series of tests employing other gases (e.g., N_2) would be enlightening.

While the model tests seemingly appear to provide a solid basis for the verification of the suitability of the existing skirt design, i.e., indicated acceptably low erosion rates, these tests have constantly failed to duplicate the low pressure high velocity and Mach number conditions to be experienced by the skirt. It is not possible at this point, on the basis of these or the earlier tests to predict with any assurance what the erosion rate will be in the actual nozzle skirt flow

regime. This statement is particularly true with regard to future higher temperature versions of the NERVA engine. As indicated earlier, to do so would require a comprehensive description of the reacting boundary layer coupled with a realistic description of the reaction mechanisms present when hydrogen impinges on a heated graphite surface.

It was the purpose of the experimental program undertaken during this contract to provide information concerning the detailed mechanisms by which hydrogen reacts with solid carbon (graphite) surfaces.

Experimental Program

Approach

In order for any experiment directed toward the investigation of the interaction of hydrogen with graphite surfaces to provide meaningful results it is mandatory that the basic physical characteristics of both the hydrogen gas and the graphite surface be known with precision and be independently controlable over a substantial range of values. An experiment so designed would then permit the pertinent parameters associated with the surface reactions to be independently varied and their effect upon the overall reaction schematic to be unambiguously assayed.

The use of a molecular beam nozzle generating a precisely controlled jet of hydrogen having known physical properties impinging on an accurately controlled graphite surface was chosen as the most straight forward means to satisfy the basic objectives of the study.

Experimental Apparatus

The experiment consisted then of four basic elements:

A. Hydrogen molecular beam nozzle
B. Graphite surface and its holder and power supply
C. Diagnostic instrumentation
D. Vacuum facility in which the experiment was conducted

The following brief description of each of these components serve to detail the salient characteristics of the experiment.

A. Hydrogen Molecular Beam Nozzle

Figure 1 is a photograph of the hydrogen molecular beam

nozzle. In the nozzle design gaseous hydrogen is introduced as shown and, by splitting the flow, is caused to enter both ends of the resistively heated rhenium nozzle tube. A small hole (31 μm diameter) drilled midway between the ends of the tube, along a radius, forms the nozzle proper.

By controlling the stagnation pressure and the stagnation temperature (by adjustment of the current level through the tube) a wide range of flow conditions could be obtained. Stagnation pressures of up to 20 atmospheres at stagnation temperatures up to 2800°K were possible, at flow rates up to a maximum (determined by the facility pumping capacity) of 10^{20} particles/sec.

The Mach numbers of the beam generated by such a nozzle were sufficiently high((0)M=10) so that for the purposes of the experiment the energy distribution could within narrow limits(ie $\pm$10%) be considered mono-enegetic. The use of an almost mono-energetic beam allows the influence of particle velocity on the overall reaction kinetic rate to be precisely determined.

B. Graphite Sample and Holder

Candidate graphite samples were mounted in a sample holder which would permit the surface to be oriented over 2 π steradians with respect to the center line of the beam. By varying the beam impingment angle the influence of surface anisotropicities upon the surface kinetics could be weighed. In addition provision was made for the samples to be resistively heated to

predetermined, controlled temperature levels to allow the influence of surface temperature to be compared with the effects of hydrogen particle energy.

C. Diagnostic Instrumentation

A series of increasingly sophisticated instrumentation was available for this study. Initial studies of surface erosion under various beam and surface conditions were to be conducted by qualitative and quantitative evaluation of the amount of material removed by the reaction process. By using these data as a guide a detailed investigation using a mass spectrometer to assess the reaction products would then permit a detailed evaluation of the specific surface reactions contributing to surface erosion.

D. Vacuum Facility

The use of a high vacuum environment was essential to this program. By maintaining the background pressure in the range $\leq 10^{-4}$ torr two important advantages were obtained; the absence of significant extraneous material that could mask the effects of the reaction was assured and the reaction could be observed free from the influence of additional interactions due to multiple collisions in the vicinity of the surface. The pumping capacity associated with the vacuum facility limits the maxium nozzle flow rate that can be used.

All experiments conducted in this program were run in the Guggenheim Physical Laboratory facility which permitted pressures of $\leq 10^{-4}$ torr to be maintained at particle flow rates of up to $10^{20} sec^{-1}$. Pressure levels below 10^{-4} torr correspond to mean

free paths in excess of one meter insuring favorable conditions for the observation of the reaction at the surface.

It should be noted that, in all but one respect, the physical characteristics of the hydrogen beam are quite similar to those anticipated to be present in the nozzle skirt of the NERVA flight engine. The one exception to this correspondence is the particle density. The hydrogen density at the surface of the graphite test sample, when being impinged upon by the beam, was on the order of 10^{13} to 10^{14} particles/cm^3 as compared to 10^{16} to 10^{17} particles/cm^3 in the actual nozzle. The simulation of nozzle skirt surface operating conditions was not the goal of this work. It is purely coincidental that the experimental parameters approximate those anticipated to be present.

Overall Progress

Considerable effort was devoted, during the early phases of the program, toward the development of a nozzle capable of providing the requisite hydrogen flows at the pressures and temperatures required for the test program. Initial attempts to produce a nozzle beam using tantalum nozzle tubes revealed that operation at modest temperatures (ie, (0) 1000°K) soon led to catastrophic failure because of embrittlement. As a consequence the use of rhenium nozzle tubes was pioneered.

A supply of vapor deposited rhenium, and tungsten - 25%, rhenium nozzle tubes were secured and tested for long term compatibility with hydrogen under conditions of interest for this experiment series. The rhenium tubes supplied by The Advanced Rocket Technology Corporation of Irvine, California

proved to be more than adequate to the task and superior to the more brittle tungsten/ rhenium alloy tubes tested.

The use of rhenium as a nozzle material necessitated the development of special drilling techniques to produce the microscopic holes required for the generation of high Mach number beams. By using specially ground tungsten carbide drill bits and a microdrilling apparatus purchased from National Jet Company of Cumberland, Maryland a number of nozzles were fabricated for use in the program.

An extensive series of tests were conducted to accurately determine the velocity distribution of the hydrogen beam produced by these nozzles when operated over a wide range of stagnation pressures and temperatures. These tests, using existing time of flight velocity distribution apparatus, revealed the Mach number to be in the range of 10 to 20 for all operating conditions and therefore adequate for the initial series of erosion tests.

The first series of tests had as its goal the qualitiative evaluation of the various molded graphite skirt materials, listed in Table 1. For these tests the unheated 2 cm x 4 cm polished samples were mounted normal to the beam center line and 5 cm from the nozzle exit plane. Meticulous attention was devoted to assuring that the test conditions were maintained the same for each sample. By operating at a stagnation temperature of 2000°K and a pressure of 3 atmospheres hydrogen

particle mean energy of 0.6 ev was obtained. Each sample was irradiated for a period of three (3) hours, during which the flow rate and particle energy was maintained constant within 2%.

A thin tantalum shadow strip was afixed across the center of the sample piece to facilitate comparison of irradiated and unexposed surfaces. Figure 2 is a photograph taken in visible light of an irradiated sample. In this photograph the light horizontal band is the unirradiated surface, the darker areas having been exposed to the hydrogen beam. The small light rectangular areas at the corners were shielded from the impinging beam by clips used to restrain the sample in the holder.

The sample shown in this photograph (Sample 172) was visually quite similar to the other seven tested. In all cases visual inspection failed to reveal any marked differences amongst the samples studied. The demarcation between irradiated and unirradiated areas of the samples studied was sharp and quite distinct even for the areas shielded by the clips whose edges were raised somewhat above the sample surface, (the tantalum shield was in direct contact with the sample surface).

Because of this unambiguous visual evidence of beam impingement induced surface alteration it was anticipated that photomicrographs taken with a scanning electron microscope (SEM) would permit a quantitative measurement of surface erosion to be made. The strategm employed was to orient the sample such that the step in the surface (viewing from the eroded,

irradiated surface toward the shielded surface) could be clearly imaged and its elevation measured.

Figure 3 is a photomicrograph of the boundary region between the irradiated area (right and below) and the shielded area (left and above) of sample 172. This material displayed the highest degree of surface alteration of all the samples studied with the SEM. In fact it was the only sample of the eight (8) tested in which it was possible to detect the boundary region at any level of magnification.

This result was most unexpected because of the exceptionally sharp, distinct visual evidence all of the samples displayed for beam induced alteration. Inspection of figure 3 and a similar photograph of this sample surface obtained at a manification of 4000X (displayed as figure 4) showed that the radiated surface has undergone what can best be described as mild excoriation. Surface irregularities in the irradiated area are observed to be softly rounded and generally subdued as compared to the shielded zone.

Close scrutiny of the photomicrographs taken of the eight (8) test samples at various view angles and at magnifications up to 4000X reveal, at most, marginal changes in the surface textures of all except #172. On the basis of this evidence the sample #172 material can be considered to be more susceptible to attack by energetic hydrogen atoms than the others tested.

This conclusion must be mollified by the realization that the surface changes apparent could very well have resulted from a process that was initially quite pronounced during the three (3)

hour test period and that no or very little change occured thereafter. The resolution of this question is a moot point pending further tests involving both shorter and longer irradiation times with higher surface temperature, higher beam particle energies and varied sample orientations.

Although planned these tests were not implemented during this contract because the overall emphasis of the program was shifted soon after the data were collected and in the process of being analyzed. At the conclusion of the reported sample test series major effort was devoted toward the refinement of the rhenium, high pressure, high temperature nozzle design. As a result of these refinements to the nozzle design stemming from an extended series of tests at temperatures in the 2600 to 2700°K range at pressures in excess of one atmosphere total nozzle longenity has been extended to 30 hours at 2700°K.

On the basis of the known crystallographic and sublimation properties of rhenium a 30 hour useful life at 2700°K corresponds to virtually indefinite (1000 hours) service life at operating temperatures below 2400°K. As a consequence a high temperature, high pressure molecular beam nozzle is now available for the acceleration of all non-oxidizing gases and vapors, a signal advance in the field of molecular beam research.

TABLE I

Manufacturing Histories of Molded Graphite (1)

TEST SAMPLES

Sample Number	Filler	Binder	Heat Treatment (C)
143 (2)	POCO PCD (-OQ)	CAI (4)	2800
152 (2)	CAI (1000 C)	ITX (4)	2800
162 (2,3)	ITX (1000)	ITX	2800
169 (2)	POCO PCD (-9) Q	ITX	2800
171 (2)	POCO PCD (-0) Q	ITX	2800
172	POCO PCD (-9) Q	Ashland 240 Pitch	2800
175	ITX (700°C)	ITX	2800
POCOAXF5Q Commercial - No History			2500

(1) Filler and binder molded at 1600 psi and 1400 °C, except for POCO AXF5Q. Heated without pressure to 2800 °C.

(2) Impregnated with CAI Polymer.

(3) Same graphite as 175 except 162 was impregnated.

(4) CAI - Cinnamylideneindene.

NOTES:

1. These materials were made for NERVA Program, SNC-95.

2. Supplied by Mr. J. M. Napier, Nuclear Division, Union Carbide Corporation P.O. Box Y, Oak Ridge, Tennessee 37830.

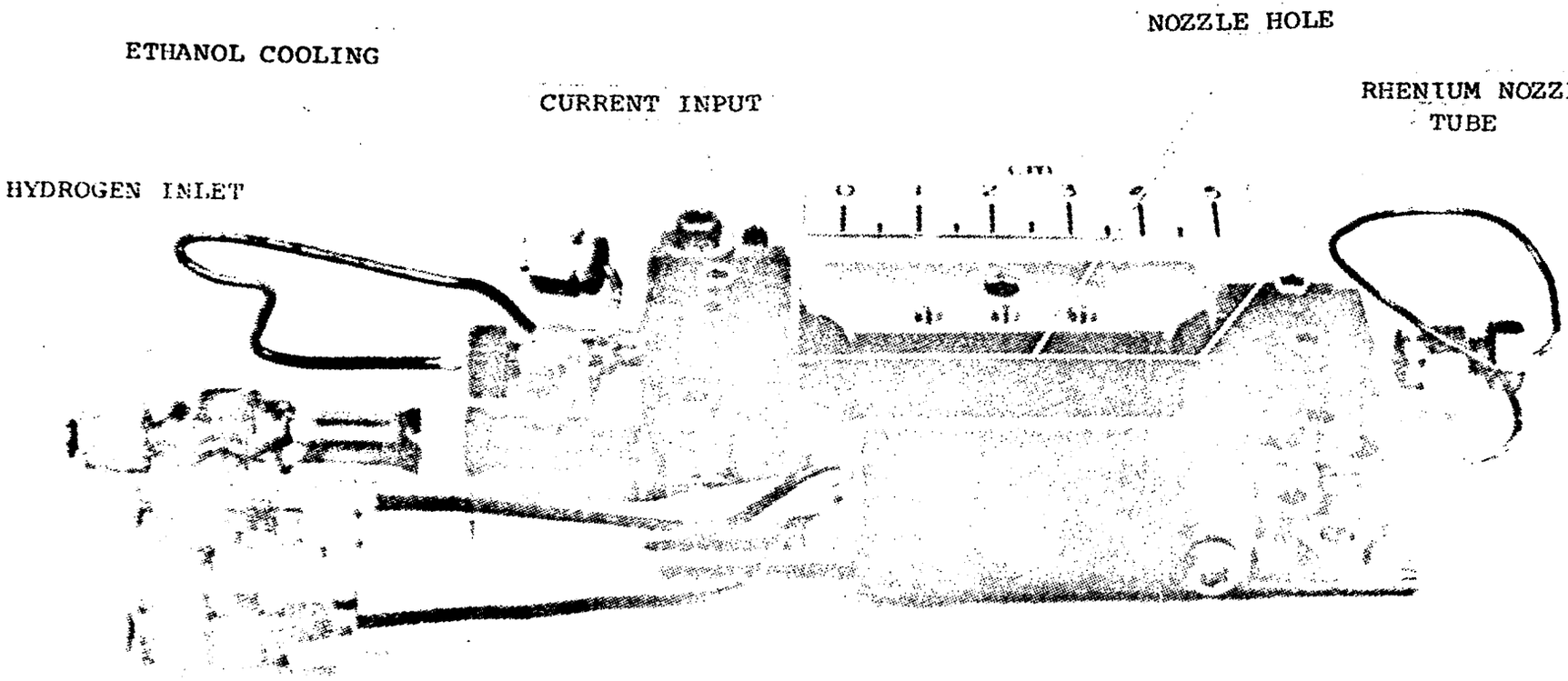

HYDROGEN MOLECULAR BEAM NOZZLE ASSEMBLY

FIGURE 1

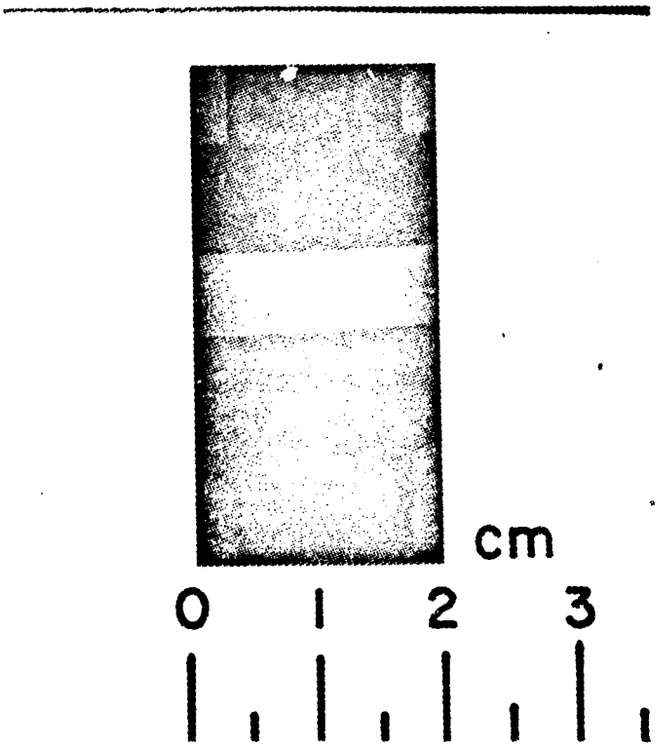

Figure 2. Photograph of graphite sample # 172.

Figure 3. Scanning Electron Microscope Photograph of Boundary between irradiated surface (on right) and shielded surface (magnification X2000)), Sample #172

Figure 4. Same as figure 3 but magnification X4000.

REFERENCES

1-1 Sharma, O. P., "Status Report on High Speed Hydrogen/Graphite Interaction," NGR 31-001-230, January 23, 1973, AMS Dept. Princeton University.

1-2 Herring, H. J. and Mellor, G. L., "A Computer Program to Calculate Laminar and Turbulent Boundary Layer Development in Compressible Flow With Heat Transfer," Princeton University, Dept. of Aerospace and Mechanical Sciences Report, June 1972.

2-1 Frey, H. M., Nickerson, G. R., and Tyson, T. J., "ODK, One-Dimensional Kinetic Reference Program," Dynamic Science, Irvine, September 1970.

2-2 Nickerson, G. R., "Striated Transonic Flow in a Converging-Diverging Nozzle," Dynamic Science, Irvine, February 1970.

2-3 Levine, J. N., e.a., "Transonic Flow in a Converging-Diverging Nozzle ' Dynamic Science, Irvine, September 1970.

2-4 Der, J. J., "Theoretical Studies of Supersonic Two-Dimensional Axisymmetric Non-Equilibrium Flow, Including Calculations of Flow Through a Nozzle," NASA TR R-164, Ames Research Center, Moffett Field, December 1963.

2-5 Frey, H. M. and Nickerson, G. R., "TDK, Two-Dimensional Kinetic Reference Program," Dynamic Science, Irvine, December 1970.

2-6 Dergazarian, T. E., e.a., "JANNAF Thermochemical Data," Thermal Laboratory, Dow Chemical Company, Midland, December 1960.

2-7 Vincenti, W. G. and Krueger, C. H., "Introduction to Physical Gas Dynamics," John Wiley and Sons, Inc., New York, August 1970.

2-8 Moretti, G. and Abbett, M., "Non-Equilibrium Effects for Quasi Equilibrium Flows in Nozzles," AIAA Paper No. 66-626, AIAA Second Propulsion Joint Specialists Conference, Colorado Springs, June 1966.

2-9 Kliegel, J. R. and Tyson, T. J., "Discussion of Chemical Kinetic Integration Techniques," WSCI Paper No. 68-45, Combustion Institute and University of California, Session on Chemical Kinetics Calculations, Berkeley, October 1968.

2-10 Eschenroeder, A. Q. and Lordi, J. A., "Catalysis of Recombination in Non-Equilibrium Nozzle Flow," 9th Symposium of Combustion

2-11 Zeleznik, F. J. and Gordon, S., "A General IBM 704 or 7090 Computer Program for Computation of Chemical Equilibrium Compositions, Rocket Performance and Chapman-Jouquet Detonations,"

NASA TN D-1454; Lewis Research Center; Cleveland; October 1962.

REFERENCES CON'T.

3-1 Altseimer, J. H., Mader, G. F., and Stewart, J. J., "Operating Characteristics and Requirements for the NERVA Flight Engine," AIAA Paper No. 70-676, AIAA 6th Propulsion Joint Specialist Conference, San Diego, California, June 15-19, 1970.

3-2 Clarke, J. T. and Fox, B. R., "Reaction of Graphite Filaments with Hydrogen Above 2000 K," J. of Chem. Phys., 46, 827, (1967)

3-3 Sanders, W. A., "Rates of Hydrogen-Graphite Reaction Between 1550 and 2260 C," Lewis Research Center, NASA TN D-2738, April 1965.

3-4 Heddon, K., "The Formation of Methane from Hydrogen and Carbon at High Temperatures and Pressures," Proc. of the Conf. on Carbon, p. 125, 1961.

3-5 Brown, R. L., "HES AGCarb-101 Erosion Test Heat Transfer Analysis," Aerojet Nuclear Systems Co., Sacramento, Internal Memo, to: Cloosen, L. B., 8 June 1970.

3-6 Williams, J. J., "AGCarb Erosion/Corrosion Sealing," (WO 1188-26-524) Aerojet Memorandum, to: Shurly, L. A., 8 June 1970.

APPENDIX A

THEORETICAL DERIVATIONS

Considering a mixture of hydrogen atoms and molecules, and defining α as the ratio of the mass of hydrogen atoms present in the mixture to the total mass of the mixture, the number densities of H and H_2 can be determined as

$$n_H = \frac{\alpha}{m_H} = \frac{2\alpha}{2m_H}$$

and

$$n_{H_2} = \frac{1-\alpha}{m_{H_2}} = \frac{1-\alpha}{2m_H}$$

where m_H is the mass of a hydrogen atom.

Using these expressions the equation of state can be written

$$\frac{p}{\rho} = kT\left(\sum_i n_i\right) = \frac{k}{2m_H}(1+\alpha)T \qquad (A1)$$

where k is the Boltzmann constant.

From equation (A1) can be deduced

$$\frac{p}{\rho} = \frac{k}{2m_H}(1+\alpha)T = \frac{\mathcal{R}}{m.w._{mixture}}T$$

Or, as

$$m.w._{mixture} = \frac{2w_H}{1+\alpha}$$

where w_H is the atomic weight of hydrogen and $\mathcal{R}$ is the universal gas constant, it follows

$$\frac{\mathcal{R}}{w_H} = \frac{k}{m_H} \qquad (A2)$$

The enthalpy is defined

$$h = \frac{p}{\rho} + e$$

where e is the specific internal energy of the mixture, with zero energy taken to be that of the atomic species at absolute zero temperature.

As only vibrational, rotational, translational and dissociation energies of the species are considered (electronic excitation is neglected), e can be written

$$e = \sum_i n_i (E_{dissociation_i} + E_{translation_i} + E_{vibration_i} + E_{rotation_i})$$

summed over both species i in the mixture.

Translation, rotation and vibration are assumed to be in equilibrium, i.e. they have a Maxwell-Boltzmann distribution.

Expressions for the energies are then

$$E_{rot_i} = kT$$

$$E_{vib_i} = \frac{k\Theta_{Vi}}{e^{\Theta_{Vi}/T} - 1}$$

$$E_{tr_i} = 3/2\ kT$$

$$E_{dis_i} = k\Theta_{Di}$$

where

Θ_{Vi} = characteristic vibrational temperature of species i

Θ_{Di} = characteristic dissociation temperature of species i.

As the atomic species has only translational energy, one obtains for the internal energy

$$e = \frac{k}{2m_H}\left(\alpha/2 + 5/2 + \frac{1-\alpha}{T}(\Theta_V/(e^{\Theta_V/T} - 1) + \Theta_D)\right)T \qquad (A3)$$

and for the enthalpy

$$h = \frac{k}{2m_H}\left(3\alpha/2 + 7/2 + \frac{1-\alpha}{T}(\Theta_V/(e^{\Theta_V/T} - 1) + \Theta_D)\right)T \qquad (A4)$$

or

$$e = e(\alpha, T)$$

$$h = h(\alpha, T)$$

Θ_V and Θ_D are the characteristic temperatures of molecular hydrogen.

For the calculation of the specific heat ratio γ and of some other quantities we will need the partial derivatives of the enthalpy.

$$\frac{\partial h}{\partial \alpha} = h_\alpha = \frac{k}{2m_H}\left[\frac{3}{2} - \frac{1}{T}\left(\frac{\Theta_V}{e^{\Theta_V/T}-1} + \Theta_D\right)\right]T \qquad (A5)$$

$$\frac{\partial h}{\partial T} = h_T = \frac{k}{2m_H}\left[\frac{3}{2}\alpha + \frac{7}{2} + (1-\alpha)\,c_6\right] \qquad (A6)$$

where

$$c_6 = \left\{\frac{\Theta_V}{T\left(e^{\Theta_V/T}-1\right)}\right\}^2 e^{\frac{\Theta_V}{T}}$$

As the specific heat at constant volume c_V is defined

$$c_V = \frac{\partial e}{\partial T} = \frac{\partial}{\partial T}\left(h - \frac{p}{\rho}\right) = h_T - R$$

where

$$R = \frac{(1+\alpha)\,\mathcal{R}}{2m_H}$$

is the specific gas constant of the mixture, and

$$\gamma = \frac{c_p}{c_V} = 1 + \frac{R}{c_V}$$

it follows

$$\gamma = \frac{1}{1 - \frac{k}{2m_H}\frac{(1+\alpha)}{h_T}} \qquad (A7)$$

For the local frozen speed of sound can now be written

$$a_f = \sqrt{\gamma RT} = \sqrt{\frac{k}{2m_H}\gamma(1+\alpha)T} \qquad (A8)$$

<u>Recombination Rate</u>

Considering the two third body reactions

$$H_2 + H \underset{k_{b_1}}{\overset{k_{f_1}}{\rightleftharpoons}} 2H + H$$

$$H_2 + H_2 \underset{k_{b_2}}{\overset{k_{f_2}}{\rightleftharpoons}} 2H + H_2$$

where

k_{f_i} = forward reaction rate of the i^{th} third body reaction

k_{b_i} = backward reaction rate of the i^{th} third body reaction,

the dissociation rate becomes (c.f. ref. 2-7)

$$\omega = \frac{d\alpha}{dt} = \left(k_{f_1}\alpha + k_{f_2}\left(\frac{1-\alpha}{2}\right)\right)\frac{\rho}{w_H}\left(1-\alpha - \frac{2\rho\alpha^2}{w_H K_c}\right) \qquad (A9)$$

where

$K_c = \frac{k_{f_i}}{k_{b_i}}$ = the equilibrium constant based on concentrations per unit volume for the reaction $H_2 \rightleftharpoons 2H$.

As the third body has no effect on the equilibrium concentrations, one can write

$$k_{f_1} = K_c\, k_{b_1} \quad \text{and} \quad k_{f_2} = K_c\, k_{b_2}$$

Substitution of these expressions in equation (A9) yields

$$\omega = K_c\left(k_{b_1}\alpha + k_{b_2}\frac{1-\alpha}{2}\right)\frac{\rho}{w_H}\left[(1-\alpha) - \frac{2\rho\alpha^2}{w_H K_c}\right] \qquad (A10)$$

Ref. 2-10 gives for the values of k_{b_1} and k_{b_2} the empirical expressions

$$k b_1 = \frac{a}{\sqrt{T}} = \frac{k_f}{2}$$

$$k b_2 = \frac{2a}{\sqrt{T}} = k_f$$

Substituting in the equation for ω, one obtains

$$\omega = \frac{\rho k_c k_f}{w_H} \left(\frac{1}{2}\alpha + \frac{1-\alpha}{2} \right) \left(1 - \alpha - \frac{2\rho\alpha^2}{w_H k_c} \right)$$

or

$$\omega = \frac{\rho k_f}{2 w_H} \left[(1-\alpha) k_c - \frac{2\rho\alpha^2}{w_H} \right]$$

As ref. 2-6 gives the equilibrium constant based on partial pressures, we will have to convert the last equation with the aid of

$$k_c = \frac{k_p^2}{\mathcal{R} T} = \frac{m_H k_p^2}{k T w_H}$$

where K_p is the equilibrium constant based on partial pressures, which results in

$$\omega = \frac{\rho k_f}{2 w_H^2} \left(\frac{m_H}{k} k_p^2 \frac{1-\alpha}{T} - 2\rho\alpha^2 \right) \qquad (A10a)$$

Eliminating ρ with the equation of state (A1) it follows

$$\omega = \left(\frac{2 m_H p}{k T (1+\alpha) w_H} \right)^2 k_f p \left\{ \frac{k_p^2}{4p} (1-\alpha^2) - \alpha^2 \right\} \qquad (A10b)$$

For equilibrium flow and chemically frozen flow the rate of dissociation is equal to zero, which gives us for frozen flow

$$f = \text{constant}$$

and for equilibrium flow

$$\frac{k_p^2}{4p}\left(1-\alpha_e^2\right)-\alpha_e^2=0$$

hence

$$\alpha_e=\sqrt{\frac{1}{1+\frac{4p}{k_p^2}}} \qquad (A11)$$

As K_p is a function of T only, α_e is a function of p and T only. The partial derivatives with respect to p and T are

$$\frac{\partial \alpha_e}{\partial p}=\frac{-2\alpha_e^3}{k_p^2} \qquad (A12a)$$

$$\frac{\partial \alpha_e}{\partial T}=\frac{4p\alpha_e^3}{k_p^2}\frac{d}{dT}(\ln k_p) \qquad (A12b)$$

<u>One-Dimensional Non-Equilibrium Flow</u>

For one-dimensional flow the equations of conservation of momentum and energy and the chemical relaxation equation can be written

$$h_T\frac{dT}{dx}+h_\alpha\frac{\omega}{w}-\frac{1}{\rho}\frac{dp}{dx}=0$$

$$\rho w\frac{dw}{dx}+\frac{dp}{dx}=0$$

$$\frac{d\alpha}{dx}=\frac{\omega}{w}$$

as shown in 2.1.1.2.

A fourth differential equation for ρ can be derived by differentiating the equation of state (A1)

$$\frac{d\rho}{dx}=\left[\frac{1}{p}\frac{dp}{dx}-\frac{1}{T}\frac{dT}{dx}-\frac{1}{1+\alpha}\frac{d\alpha}{dx}\right]\rho$$

Rearranging these equations

$$\frac{dw}{dx} = f_1 = -\frac{1}{\rho w}\frac{dp}{dx}$$

$$\frac{d\alpha}{dx} = f_2 = \frac{\omega}{w}$$

$$\frac{dT}{dx} = \left[\frac{1}{\rho T h_T}\frac{dp}{dx} - \frac{h_\alpha}{h_T}\frac{1}{T}\frac{\omega}{w}\right] T$$

$$\frac{d\rho}{dx} = \left[-\frac{1}{T_\rho}\frac{dT}{dx} + \frac{1}{p}\frac{dp}{dx} - \frac{1}{1+\alpha}\frac{\omega}{w}\right]\rho$$

Combining equations (A1) and (A7) γ can be written

$$\gamma = \frac{1}{1 - \frac{p}{\rho T h_T}}$$

or

$$\rho T h_T = \frac{\gamma p}{\gamma - 1}$$

Substituting this result in the expressions for the functions f_1, f_2, f_3 and f_4 and rearranging them

$$f_1 = \frac{-1}{\rho w}\frac{dp}{dx} \tag{A13}$$

$$f_2 = \frac{\omega}{w} \tag{A14}$$

$$f_3 = \left[\frac{\gamma - 1}{\gamma p}\frac{dp}{dx} - B\right] T \tag{A15}$$

$$f_4 = \left[\frac{1}{\gamma p}\frac{dp}{dx} - A\right]\rho \tag{A16}$$

where

$$B = \frac{h_\alpha}{T h_T} f_2 \tag{A17}$$

$$A = \frac{f_2}{1+\alpha} - B \tag{A18}$$

For the computation of the one-dimensional non-equilibrium flow we will need the partial derivatives of the functions f_i, B and A with respect to x, w, α, T and ρ.

Defining

$$c_2 = \frac{\rho k_f k_p^2 (1-\alpha)}{T} \frac{m_H}{2w_H^2}$$

$$c_3 = \frac{\rho^2 k_f \alpha^2}{w_H^2}$$

$$c_4 = \frac{1}{k_f} \frac{dk_f}{dT}$$

$$c_5 = \frac{1}{k_p} \frac{dk_p}{dT}$$

$$c_7 = \frac{h_{T\alpha}}{h_T} = \frac{1}{h_T}\left[\frac{k}{2m_H}\left(\frac{3}{2}\alpha - c_6\right)\right]$$

$$c_8 = \frac{h_{\alpha T}}{h_\alpha} = \frac{1}{h_\alpha}\left[\frac{k}{2m_H}\left(\frac{3}{2} - c_6\right)\right]$$

$$c_9 = \frac{h_{TT}}{h_T} = \frac{c_6}{T} \frac{k(1-\alpha)}{2m_H}\left[\frac{\theta_v}{T}\frac{\tau+1}{\tau-1} - 2\right] \quad ; \quad \tau = e^{\frac{\theta_v}{T}}$$

and setting

$$\frac{\partial}{\partial y_j} f_i = f_{i_{y_j}} \quad , \quad y_j = x, \alpha, w, T \text{ and } \rho$$

these derivatives can easily be shown to be

$$f_{1_x} = -\frac{1}{\rho w} \frac{d^2 p}{dx^2} \qquad (A13)$$

$$f_{1_w} = -\frac{f_1}{w}$$

$$f_{1_T} = 0$$

$$t_{1_\alpha} = 0$$

$$t_{1_g} = -\frac{t_1}{g}$$

$$t_{2_\alpha} = 0 \qquad \text{(A 14)}$$

$$t_{2_w} = -\frac{t_2}{w}$$

$$t_{2_\alpha} = \frac{-1}{w}\left[\frac{c_2}{1-\alpha} + \frac{2c_3}{\alpha}\right]$$

$$t_{2_T} = \frac{1}{w}\left[\left(c_4 + 2c_5 - \frac{1}{T}\right)c_2 - c_4 c_3\right]$$

$$t_{2_g} = \frac{1}{gw}\left[c_2 - 2c_3\right]$$

$$B_w = -\frac{B}{w} \qquad \text{(A 17)}$$

$$B_\alpha = \left(\frac{t_{2\alpha}}{t_2} - c_7\right)B$$

$$B_T = \left(c_8 + \frac{t_{2T}}{t_2} - c_9 - \frac{1}{T}\right)B$$

$$B_g = \frac{t_{2g}}{t_2}B$$

$$B_\alpha = 0$$

$$A_\alpha = 0 \qquad \text{(A18)}$$

$$A_w = -\frac{A}{w}$$

$$A_\alpha = \frac{t_{2\alpha}}{1+\alpha} - \frac{t_2}{(1+\alpha)^2} - B_\alpha$$

$$A_T = \frac{t_{2T}}{1+\alpha} - B_T$$

$$A_\rho = \frac{t_{2\rho}}{1+\alpha} - B_\rho \qquad (A15)$$

$$t_{3_u} = \frac{\gamma-1}{\gamma P}\left[\frac{d^2p}{dx^2} - \frac{1}{P}\left(\frac{dp}{dx}\right)^2\right] T$$

$$t_{3_w} = -B_w T$$

$$t_{3_\alpha} = T\left[\frac{1}{\gamma^2 P}\left(\frac{dp}{dx}\right)\gamma_\alpha - B_\alpha\right]$$

$$t_{3_T} = \frac{t_3}{T} + T\left[\frac{1}{\gamma^2 P}\left(\frac{dp}{dx}\right)\gamma_T - B_T\right]$$

$$t_{3_\rho} = -T B_\rho$$

$$t_{4_u} = \frac{\rho}{\gamma P}\left[\frac{d^2p}{dx^2} - \frac{1}{P}\left(\frac{dp}{dx}\right)^2\right] \qquad (A16)$$

$$t_{4_w} = -A_w \rho$$

$$t_{4_\alpha} = -\rho\left[\frac{\gamma_\alpha}{\gamma^2 P}\left(\frac{dp}{dx}\right) + A_\alpha\right]$$

$$t_{4_T} = -\rho\left[\frac{\gamma_T}{\gamma^2 P}\left(\frac{dp}{dx}\right) + A_T\right]$$

$$t_{4_\rho} = \frac{t_4}{\rho} - \rho A_\rho$$

The derivatives γ_T and γ_α of the specific heat ratio can be shown to be from equation (A7)

$$\gamma_\alpha = \gamma\left[\frac{k}{2m_H}\frac{\gamma}{h_T} - (\gamma-1)c_\rho\right]$$

$$\gamma_T = \gamma(1-\gamma)c_\rho$$